Extremophiles (2019) 23:219–227
https://doi.org/10.1007/s00792-019-01075-x

ORIGINAL PAPER

Physico-chemical approach to adhesion of *Alicyclobacillus* cells and spores to model solid materials

Jan Strejc[1] · Lucie Kyselova[1] · Anna Cadkova[1] · Tomas Potocar[1] · Tomas Branyik[1]

Received: 14 November 2018 / Accepted: 4 January 2019 / Published online: 17 January 2019
© Springer Japan KK, part of Springer Nature 2019

Abstract

Acidothermophilic bacteria of the genus *Alicyclobacillus* are frequent contaminants of fruit-based products. This study is the first attempt to characterize the physico-chemical surface properties of two *Alicyclobacillus* sp. and quantify their adhesion disposition to model materials [diethylaminoethyl (DEAE), carboxyl- and octyl-modified magnetic beads] representing materials with different surface properties used in the food industry. An insight into the mechanism of adhesion was gained through comparison of experimental adhesion intensities with predictions of a colloidal interaction model (XDLVO). Experimental data (contact angles, zeta potentials, size) on interacting surfaces (cells and materials) were used as inputs into the XDLVO model. The results revealed that the most significant adhesion occurred at pH 3. Adhesion of both vegetative cells and spores of two *Alicyclobacillus* sp. to all materials studied was the most pronounced under acidic conditions, and adhesion was influenced mostly by electrostatic attractions. The most intensive adhesion of vegetative cells and spores at pH 3 was observed for DEAE followed by hydrophobic octyl and hydrophilic carboxyl surfaces. Overall, the lowest rate of adhesion between cells and model materials was observed at an alkaline pH. Consequently, prevention of adhesion should be based on the use of alkaline sanitizers and/or alkaline rinse water.

Keywords *Alicyclobacillus* sp. · Cell adhesion · Model materials · Surface interaction · XDLVO model

Introduction

Alicyclobacillus species are regarded as a serious cause of spoilage in the worldwide fruit juice industry (Steyn et al. 2011; Tianli et al. 2014; Azeredo et al. 2016). Members of *Alicyclobacillus* are rod-shaped, thermoacidophilic, aerobic, nonpathogenic endospore-forming bacteria that contain unique ω-alicyclic fatty acids as principal membrane lipid components and can grow over wide temperature (20–70 °C) and pH ranges (2.0–6.0) (Steyn et al. 2011; Tianli et al. 2014; Huang et al. 2015a). Undesirable spoilage caused by *Alicyclobacillus* is characterized by a specific off-flavour described as smoky, phenolic, or medicinal, with or without visible cloudiness (Chang and Kang, 2004; Smit et al. 2011; Steyn et al. 2011). The lack of typical gas production that can swell a container makes early detection of contamination difficult (Pettipher et al. 1997). The predominant metabolites associated with *Alicyclobacillus* spoilage are guaiacol, 2,6-dibromophenol and 2,6-bichlorophenol (Huang et al. 2015a).

The major source of contamination is usually garden soil from which bacteria and their spores are spread to the fruit or cleaning water used during processing (Chen et al. 2006; Huang et al. 2015a). Acidophilic properties of these microorganisms allows them to thrive in the highly acidic environment of fruit beverages or concentrates (Chang and Kang, 2004; McKnight et al. 2010; Spinelli et al. 2010). Moreover, thermophilic properties, in combination with sporulation and biofilm production, enables them to survive harsh processing conditions such as washing, sanitizers or the hot-fill and hold pasteurization process (88–96 °C, 2 min) (dos Anjos et al. 2013; Tianli et al. 2014).

Microbial biofilm formation is a dynamic multistage process gradually leading to irreversible adhesion of microorganisms to a surface, depending on contact surface properties, environmental conditions, and extracellular polymers

Communicated by A. Driessen.

✉ Tomas Branyik
tomas.branyik@vscht.cz

[1] Department of Biotechnology, University of Chemistry and Technology Prague, Technicka 5, 166 28 Prague, Czech Republic

secreted by bacteria (e.g. polysaccharides, proteins, lipids, DNA) (Sauer 2003; Srey et al. 2013). During biofilm development, diversification of cell function occurs (Olszewska 2013) and the ideal environment for sporulation is created (spores are located in the upper layers) (Abee et al. 2011). Cells in the biofilm exhibit coordinated group behaviour that increases their resistance towards external factors, cleaning and antimicrobial agents. The biofilm thus represents an elevated risk of spreading contamination across production facilities (Frank 2000; Peng et al. 2002). Although studies on *Alicyclobacillus* adhesion and biofilm production on abiotic surfaces are still limited, it has been already shown that this bacterial taxon has the ability to build biofilms on stainless steel, nylon and PVC (dos Anjos et al. 2013; do Prado et al. 2018), and to a lesser extent on glass slides (Tyfa et al. 2015).

The goal of this work was to characterize the surface properties of *Alicyclobacillus acidoterrestris* CCM 4660 and *Alicyclobacillus sacchari* DSM 17974 vegetative cells and spores. Furthermore, their interactions were studied with solid model materials mimicking the main types of materials occurring in the food industry. Experimental adhesion data were compared with model predictions of XDLVO theory to identify the main driving forces for cell adhesion and to describe conditions that favour adhesion.

Materials and methods

Microorganisms and magnetic beads

The *Alicyclobacillus* strains used in this study were *A. acidoterrestris* CCM 4660 and *A. sacchari* DSM 17974. Three types of magnetic beads (SiMAG-ionex, 0.5 µm diameter, Chemicell, Germany) carrying defined functional groups, i.e. DEAE (diethylaminoethyl), carboxyl and octyl, were used as model materials to contact *Alicyclobacillus* cells.

Cultivation

Cultivation medium (CM) of the following composition was used (in g l^{-1}): yeast extract (6.0, Alfa Aeasar, USA), glucose (5.0, Penta, Czech Republic), $CaCl_2 \cdot 2H_2O$ 0.25 g l^{-1}, $MgSO_4 \cdot 7H_2O$ 0.5 g l^{-1}, $(NH_4)_2SO_4$ 0.2 g l^{-1}, KH_2PO_4 3.0 g l^{-1} (all salts from Penta, Czech Republic) and the pH was adjusted to 4. Cultivation of vegetative cells was carried out in 500 mL Erlenmeyer flasks (250 mL medium; 150 rpm; 48 h; 45 °C). After cultivation, a cell suspension was obtained by washing twice with distilled water and centrifuging (6000 rpm; 5 min). For cultivation of spores, agar 30.0 g l^{-1} (Sigma-Aldrich) and $MnSO_4 \cdot H_2O$ 0.01 g l^{-1} (Lach-Ner s.r.o., Czech Republic) were added into the CM. A suspension of vegetative cells was spread on agar plates and allowed to grow for 72 h at 45 °C to reach > 90% of spores in the cell count, as observed microscopically after the Wirtz-Conklin method of staining (Hamouda et al. 2002). From the agar plates, spores were removed with an inoculating loop, resuspended, washed twice with distilled water, centrifuged (3000 rpm; 3 min) and immediately used for subsequent tests (image analysis, contact angle, and zeta potential measurements, adhesion tests).

Image analysis

Pictures of vegetative cells and spores of *Alicyclobacillus* strains were taken using an Olympus BX51 microscope with Olympus C5050 digital camera. For cell size determination, ImageJ (NIH, USA) software was used. Vegetative cells were evaluated after growth in CM for 48 h at 45 °C, while spore size was evaluated after 72 h growth on agar plates at 45 °C.

Contact angles' measurement

Contact angle measurements were carried out by the sessile drop technique on a CAM 200 goniometer (KSV Instruments, Finland). Drops (volume ≈ 3 µl) of water, formamide and 1-bromonaphthalene (all from Sigma-Aldrich) were measured 1 s after placement, ten times for each sample, at 25 °C. For the contact angle measurement, a smooth layer of cells was deposited on a membrane filter (47 mm diameter, 0.45 µm pore size, Whatman, USA) under negative pressure using 0.26 mg of dry biomass per cm^2 of filter area. The cell lawns were then deposited on agar plates to stabilize their moisture content, fixed on a microscope glass slide, and allowed to dry for 40 min at 25 °C (Sharma and Hanumantha Rao 2002). The surface properties of magnetic beads (MB) were characterized by contact angles (CA) in the form of compressed pellets. Pellets were prepared from 0.05 g of dry MB by pressing (7 MPa, evacuable pellet press 13 mm, Pike Technologies).

Zeta potential measurement

Zetasizer Nano-ZS (Malvern, UK) and calculations according to the Smoluchowski equation were used for zeta potential measurements. Measurements were carried out in a model environment (10 mM KCl, pH 3-12) and each sample was measured nine times. Sample concentrations (in dry weight) were adjusted to 27 mg l^{-1} for cells and to 20 mg l^{-1} for MB.

Model calculations

Two physico-chemical approaches were used for prediction of interaction intensities between cells and magnetic

particles. Total free energies of interaction were calculated from CA values (Table 1) according to the thermodynamic approach (van Oss 1995). For colloidal interactions, the extended DLVO theory was used (van Oss 2003). Predictions according to XDLVO theory were calculated for model environments (10 mM KCl, pH 3–12), the Hamaker constant was estimated from the ΔG^{LW} values (Table 2), the characteristic decay length for acid–base (AB) interactions was 0.6 nm (van Oss 2006), and the intensity of AB interactions was expressed using ΔG^{AB} values (Table 2).

Adhesion tests

Adhesion between cells and MB was tested in defined model environments similar to a previously described procedure (Prochazkova et al. 2013). Cell suspensions (2 ml) of a defined concentration (0.3 ± 0.03 g l^{-1}) in electrolyte (10 mM KCl, pH 3–12) were mixed (5 rpm, orbital mode, Hulamixer, Invitrogen, USA) with specific amounts of MB for 10 min in plastic test tubes. Subsequently, MB were exposed to an NdFeB magnet (25 × 10 mm, Neomag, Czech Republic) for 10 min followed by measurement of supernatant absorbance (600 nm). Adhesion intensity (AI %) was calculated according to the equation: $AI = [(A_0 - A_1)/A_0] \times 100$, where A_0 is the absorbance of the cell suspension and A_1 is the absorbance of the supernatant after accelerated magnetic sedimentation. Due to the small size of *Alicyclobacillus*, self-sedimentation of cells was negligible. All experiments were performed in triplicate and results are presented as mean values.

Results

Physico-chemical surface properties of cells and magnetic beads

The average ZP values of bacteria, as a function of pH in a symmetrical model electrolyte (10 mM KCl) indicate that both the vegetative cells and spores were electronegative over the whole pH range (Fig. 1). Under pH neutral and acidic conditions, the spores of both strains had the most

Table 1 Average contact angles, total surface tensions (γ^{TOT}) and their apolar (γ^{LW}) and polar (γ^{AB}) components and total free energies of interaction (ΔG^{TOT}) for the system surface–water–surface (SWS) of *A. acidoterrestris* CCM 4660, *A. sacchari* DSM 17974 and magnetic beads

Surfaces	Contact angle (°)			Surface tension[a]			ΔG^{TOT} (SWS)[b]
	W	*F*	*B*	γ_{LW}	γ_{AB}	γ_{TOT}	
Vegetative cells							
CCM 4660	23.4 ± 2.8	31.3 ± 3.1	38.9 ± 2.5	35.1	12.9	48.0	37.6
DSM 17974	20.5 ± 2.3	39.5 ± 2.4	41.6 ± 2.3	33.9	6.9	40.8	54.9
Spores							
CCM 4660	44.4 ± 1.1	42.9 ± 2.8	62.7 ± 1.0	23.6	20.7	44.3	15.5
DSM 17974	53.0 ± 4.3	84.1 ± 2.7	48.5 ± 4.4	30.7	46.6	77.3	37.5
Magnetic beads							
DEAE	65.2 ± 1.3	27.7 ± 1.3	15.8 ± 1.1	42.7	8.3	51.0	− 40.8
Carboxyl	31.9 ± 1.2	20.6 ± 0.5	11.5 ± 0.1	43.5	10.7	54.2	15.3
Octyl	80.2 ± 1.9	33.0 ± 1.6	15.2 ± 0.2	42.9	2.0	44.9	− 64.8

W water, *F* formamide, *B* 1-bromonaphthalene

[a]Units in mJ/m^2

Table 2 Total free energies of interaction (ΔG^{TOT}) and their apolar (ΔG^{LW}) and polar (ΔG^{AB}) components as calculated according to the thermodynamic balance of interaction energies for the system cell–water–surface (CWS) consisting of either *A. acidoterrestris* CCM 4660 or *A. sacchari* DSM 17974 cells and one type of the magnetic bead (DEAE, carboxyl or octyl)

Interaction system	Free energy of interaction (mJ/m^2)					
Cell–water–surface (CWS)	Vegetative cells			Spores		
	ΔG^{LW}	ΔG^{AB}	ΔG^{TOT}	ΔG^{LW}	ΔG^{AB}	ΔG^{TOT}
CCM 4660-W-DEAE	− 4.7	− 3.4	− 8.1	− 0.7	− 8.4	− 9.1
DSM 17974-W-DEAE	− 4.3	− 0.9	− 5.2	− 3.2	15.6	12.4
CCM 4660-W-carboxyl	− 4.8	31.8	27.0	− 0.7	18.8	18.1
DSM 17974-W-carboxyl	− 4.5	38.7	34.2	− 3.3	40.0	36.7
CCM 4660-W-octyl	− 4.7	− 22.2	− 26.9	− 0.7	− 23.2	− 23.9
DSM 17974-W-octyl	− 4.3	− 21.9	− 26.2	− 3.3	3.2	− 0.1

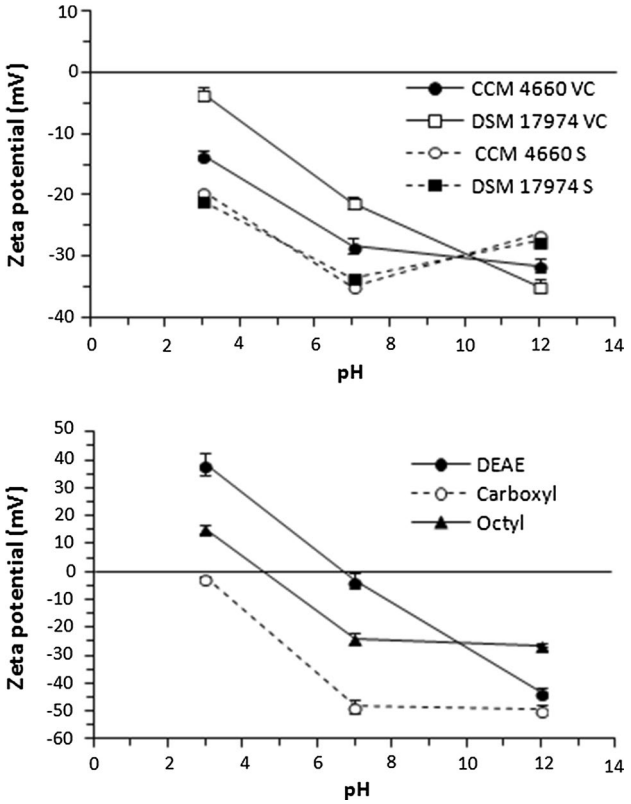

Fig. 1 Zeta potential of *A. acidoterrestris* CCM 4660, *A. sacchari* DSM 17974 and magnetic beads in electrolyte (10 mM KCl) as a function of pH

negative ZP, while at pH 12 the vegetative cells of strain *A. sacchari* DSM 17974 had the lowest ZP.

The ZP of MB functionalized with DEAE and octyl groups showed an ionex character dependent on the pH of the environment. At pH 3 the DEAE and octyl MB carried a positive charge up until isoelectric points (pI) 6.8 and 4.6, respectively. The same surfaces above pI had negative ZPs, including the carboxyl MB over the whole pH range studied (Fig. 1).

Hydrophilic surfaces are characterized by $\gamma^{LW} \approx 40$ mJ m^{-2}, $\gamma^{+} \approx 0$ mJ m^{-2}, and $\gamma^{-} > 28$ mJ m^{-2}, as well as positive ΔG^{TOT}, when considering surface–water–surface (SWS) interactions in water (van Oss 1995). Calculations of surface tensions revealed similar hydrophilic and prevailing electron donor characteristics ($\gamma^{-} = 56$–66 mJ m^{-2}, $\gamma^{+} = 0.17$–0.74 mJ m^{-2}) for vegetative cells of both *Alicyclobacillus* strains. The hydrophilic character of vegetative cells can also be seen from positive ΔG^{TOT} values (Table 1). Spores of *A. acidoterrestris* CCM 4660 and *A. sacchari* DSM 17974 have nonzero γ^{+} (2.8 and 6.7 mJ m^{-2}, respectively) and they are prone to provide more polar interactions (higher γ_{AB}) than vegetative cells (Table 1). However, from the point of view of total free energies of interaction, sporulation resulted in fewer hydrophilic surfaces (lower ΔG^{TOT}) for both strains (Table 1). The higher values obtained for γ^{-} as compared to γ^{+} are not surprising, since the ZP measurements showed predominantly negative surface charges on both vegetative cells and spores of *Alicyclobacillus* strains (Fig. 1).

The low CA values for bromonaphthalene on lawns of MB and their high γ^{LW} indicate a greater propensity to provide apolar interactions, as compared to bacterial cells. The free energy of interaction values (ΔG^{TOT}) between MB indicate a different wettability. Octyl and DEAE MB, according to ΔG^{TOT}, were hydrophobic, whereas carboxyl MB had a hydrophilic character. The surface hydrophobicity of MB used increased in the order carboxyl < DEAE < octyl (Table 1).

Prediction of cell–surface interactions

For some combinations of vegetative cells, spores and favorable model materials (positive) an adhesion energy balance of $\Delta G^{TOT} < 0$ was obtained, whereas for other materials, the balance was unfavourable ($\Delta G^{TOT} > 0$) (Table 2). Comparing the total free adhesion energies (Table 2) with real adhesion experiments (Fig. 3), the thermodynamic approach was not able to discriminate sufficiently the colonization of model materials by *Alicyclobacillus* strains. Since the thermodynamic model was not able to provide a generalized description of bacterial adhesion to model materials, the extended DLVO (XDLVO) theory was used. This combines the classical non-covalent Liftshitz-van der Waals (LW) and electrostatic (EL) interactions with Lewis acid–base (AB) interactions (van Oss 2003).

For XDLVO calculations, the diameter of the MB (0.5 µm) was used as given by the manufacturer. Image analysis was performed for determining the size of vegetative cells and spores of *Alicyclobacillus* strains. Vegetative cells of *A. acidoterrestris* CCM 4660 and *A. sacchari* DSM 17974 had the following mean lengths, 4 ± 1.7 and 3.4 ± 0.6 µm, and mean diameters, 0.95 ± 0.15 and 0.8 ± 0.2 µm, respectively. In the case of vegetative cells, the mean diameter of rods was chosen as the characteristic size, based on an approximation of the geometry of crossed cylinders (Israelachvili, 2011). The spores of *A. acidoterrestris* CCM 4660 and *A. sacchari* DSM 17974 had the shapes of oblate spheroids, of mean lengths 1.42 ± 0.12 and 1.57 ± 0.16 µm, mean widths 0.7 ± 0.06 and 0.65 ± 0.07 µm and circularities 0.69 ± 0.04 and 0.69 ± 0.1, respectively. In the case of spores, the applied interaction geometry for XDLVO calculations was sphere–sphere.

The simulation of total interaction energies (G_{XDLVO}) between vegetative cells/spores and MB, as a function of the separation distance at different pH values, predicted either the absence or presence of potential energy barriers at close contact (collision) of interacting entities (Fig. 2).

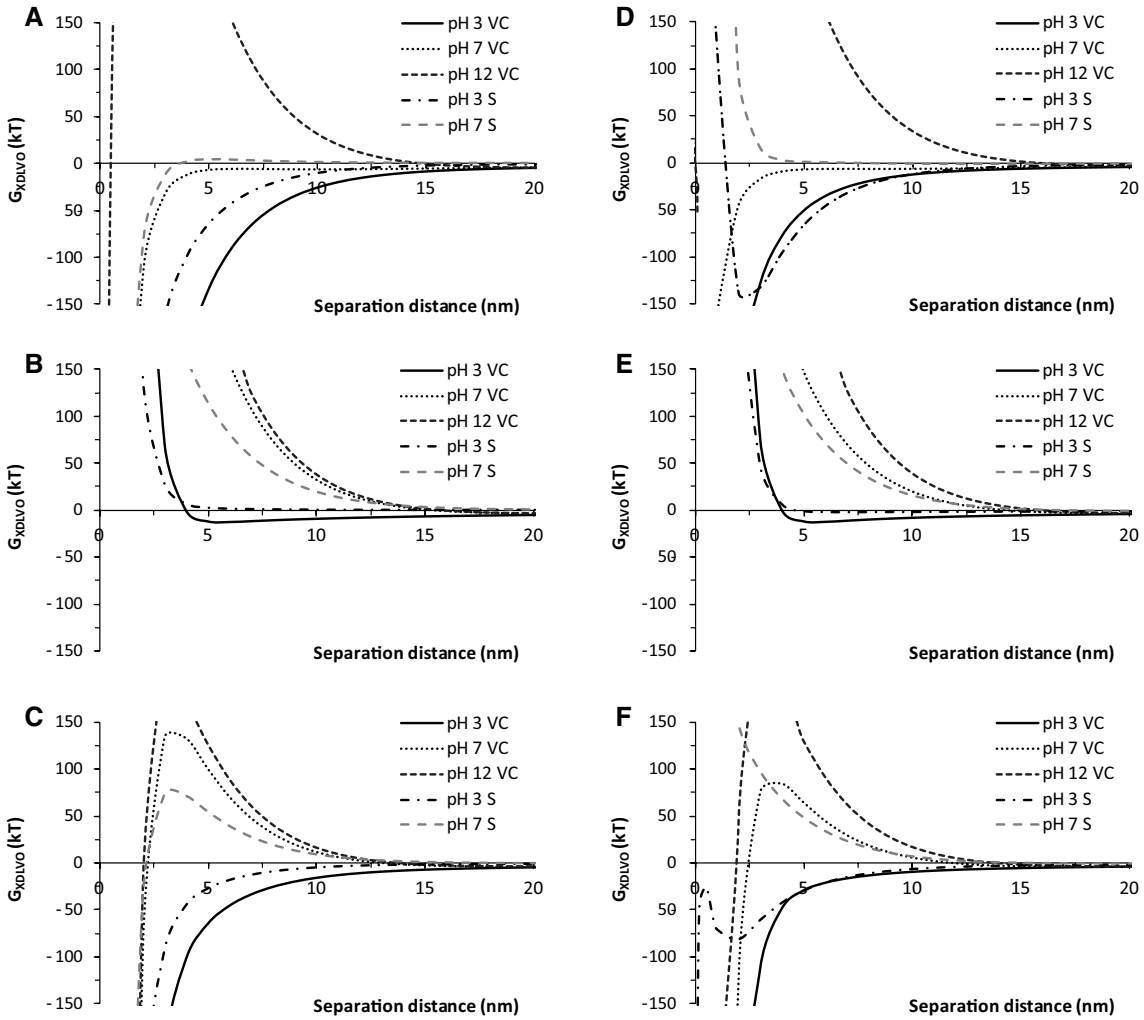

Fig. 2 Total interaction energy (G_{XDLVO}) as a function of the separation distance between *A. acidoterrestris* CCM 4660 (**a**–**c**), *A. sacchari* DSM 17974 (**d**–**f**) vegetative cells (VC) or spores (S) and DEAE (**a**, **d**), carboxyl (**b**, **e**) or octyl (**c**, **f**) magnetic beads in electrolyte (10 mM KCl) at different pHs according to the XDLVO theory

The absence of an energy barrier preventing the collision of cells with MB was predicted for the interaction of vegetative cells of both strains with DEAE MB (pH 3 and 7, Fig. 2a, d) and octyl MB (pH 3, Fig. 2c, f). For the interaction of spores, the absence of energy barriers was predicted for both strains vs. octyl MB (pH 3, Fig. 2c, f), while for DEAE MB this applied only for strain *A. acidoterrestris* CCM 4660 (pH 3, Fig. 2a).

Although direct contact is unlikely when there is an energy barrier, the interaction of vegetative cells/spores with MB can take place in a so called secondary potential minimum (Redman et al. 2004). The existence of these favorable energy minima was predicted by the XDLVO model (Fig. 2). The deepest secondary minimum (SM) was predicted for interactions of spores of *A. sacchari* DSM 17974 with DEAE MB at pH 3 and was − 139 kT. Under these conditions, the contribution of the EL and LW interaction forces to overall interactions were attractive, while the AB interactions were repulsive.

Shallow SMs (− 1 to − 13 kT) were predicted for the interaction of vegetative cells and spores of both strains with carboxyl MB at pH 3 (Fig. 2b, e). During this interaction the XDLVO model predicted repulsive AB and EL and attractive LW forces at close contact of surfaces. At pH 12, significant energy barriers were predicted for the interaction of vegetative cells with all MB (Fig. 2) due to strong electrostatic repulsion between interacting entities.

Adhesion tests and their comparison with XDLVO predictions

Adhesion of vegetative cells/spores to MB was dependent on the ratio of interacting entities and the pH of the environment. In all situations tested, adhesion increased with

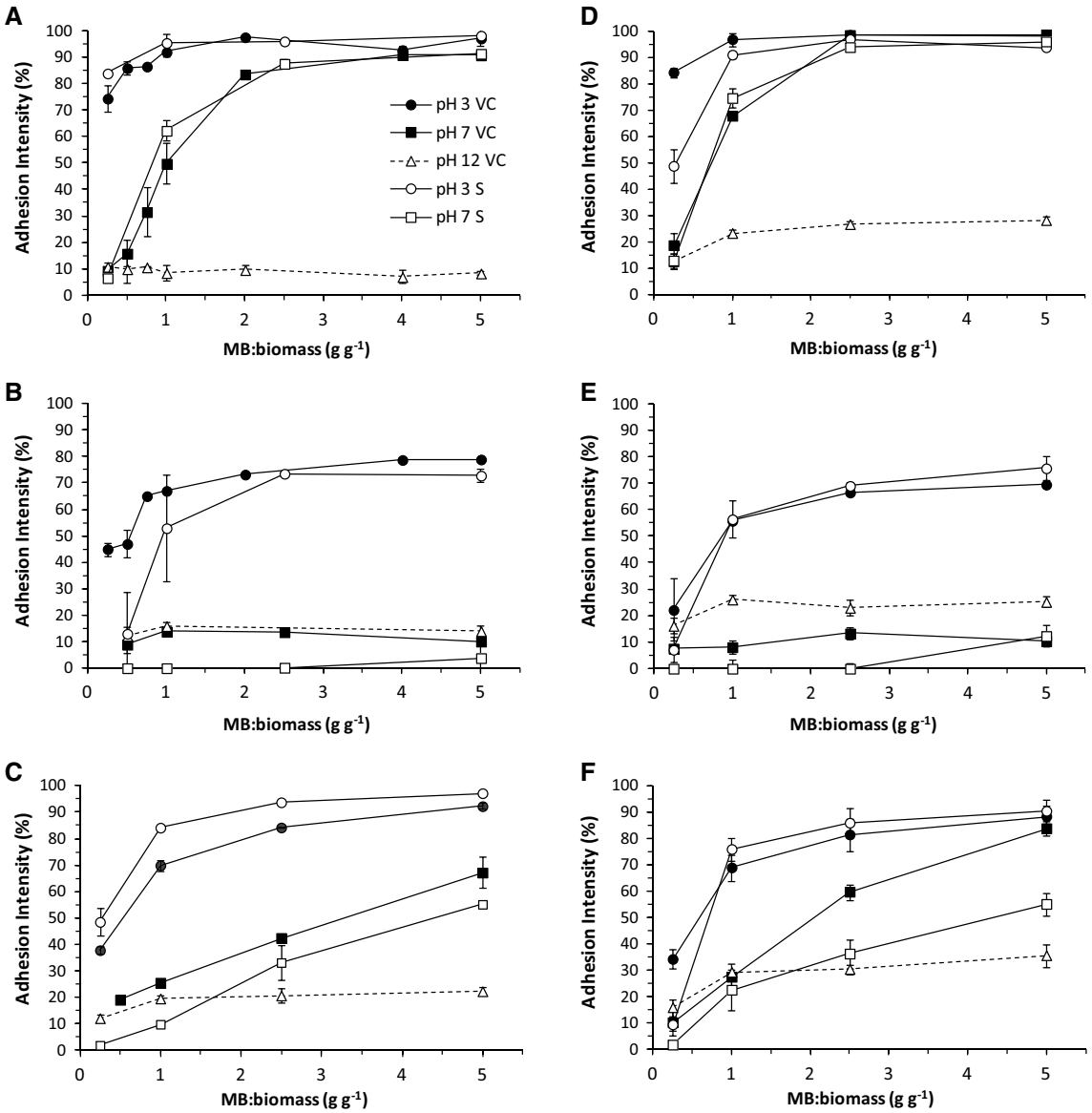

Fig. 3 Adhesion intensity of *A. acidoterrestris* CCM 4660 (**a**–**c**), *A. sacchari* DSM 17974 (**d**–**f**) vegetative cells (VC) or spores (S) to DEAE (**a**, **d**), carboxyl (**b**, **e**) or octyl (**c**, **f**) magnetic beads in electrolyte (10 mM KCl) at different pHs and different MB-to-biomass ratios

increasing MB-to-biomass ratio, often reaching a plateau (Fig. 3). In general, significant adhesion of vegetative cells/spores to MB was observed at an acidic pH. Conversely, the interaction between MB and vegetative cells at pH 12 was the weakest, with the exception of carboxyl MB at pH 7 (Fig. 3b, e). In some cases, adhesion intensity reached high levels (94–98%), such as for interaction of DEAE MB with vegetative cells and spores of both *Alicyclobacillus* strains at pH 3 (Fig. 3a, d).

A clear relationship was seen between AI (Fig. 3) and the absence of deep SM, as predicted by the XDLVO model (Fig. 2). Under conditions allowing stronger interactions (absence of an energy barrier or deep SM), the MB-to-biomass ratio resulting in high AI was lower. For example, to remove almost 100% of *A. acidoterrestris* CCM 4660 vegetative cells at pH 3 by adhesion to DEAE MB, it was necessary to achieve a MB-to-biomass ratio of 2 g g^{-1} (Fig. 3a). In this situation, the XDLVO theory predicts the absence of an energy barrier (Fig. 2a). Similarly, DEAE MB-to-biomass ratio of 5 g g^{-1} resulted in only 25% adhesion of vegetative cells of *A. sacchari* DSM 17974 at pH 12 (Fig. 3d). Accordingly, under these conditions, the XDLVO theory predicted a potential energy barrier preventing the DEAE MB interaction with *A. sacchari* DSM 17974 (Fig. 3a). The less pronounced SM predicted for cell and spore interactions with carboxyl MB (Fig. 2b, e) was

mirrored in either lower AI (max. 78%) or higher MB-to-biomass ratio required to achieve high AI (Fig. 3b, e). The energy barriers predicted (80–140 kT) for cell and spore interactions with octyl MB at pH 7 (Fig. 2c, f) were also reflected in adhesion tests with a higher MB-to-biomass ratio required to achieve high AI (Fig. 3c, f).

A more significant discrepancy between prediction and experimentation appeared only in the case of *A. sacchari* DSM 17974 spore adhesion to DEAE MB at pH 7. In this case, the XDLVO model predicted a shallow SM (− 1.5 kT at 13 nm) followed by an energy barrier at a shorter separation distance (Fig. 2d). Simultaneously the AI was comparable with vegetative cells (pH 7, Fig. 3d), for which the prediction was without energy barrier (Fig. 2d).

Discussion

Alicyclobacillus is an important member of the group of spoilage bacteria in the fruit juice industry (Azeredo et al. 2016). Members of this genus enter food processing plants on the surface of fruits. Their subsequent expansion onto the surface of processing hall floors, drainage and water systems and onto machinery in the form of biofilms was hypothesized (dos Anjos et al. 2013). A prerequisite for contamination by *Alicyclobacillus* bacteria is their presence in multispecies biofilms as a consequence of their adhesion to solid surfaces. Two spoilage routes from biofilm to target sites can be assumed (1) spreading of cells through an aqueous environment, and (2) transfer of cells in aerosols.

This work describes the adhesion of two *Alicyclobacillus* strains to model solid materials. The surface properties of model materials, represented by MB coated with different functional groups, were designed to cover the widest possible range of surface properties. Carboxyl MB were selected to represent hydrophilic surfaces, such as ceramics and glass possessing negative ZP. DEAE MB were designed to imitate stainless steel used as construction material in the food/beverage industry, having a positive ZP in an acidic environment and hydrophobic surface properties (Gispert et al. 2008; Huang et al. 2015b). Finally the modification of MB with octyl groups was selected to prepare a hydrophobic model surface representing synthetic polymers, rubbers, lubricants etc. (Bittner et al. 2017). The experimental conditions for this study simulated different scenarios, where pH 3 and 10 were chosen to mimic acidic and alkaline conditions used during sanitation and cleaning procedures in the food industry, respectively. Neutral pH 7 was chosen to mimic the rinsing of machinery and floors with water.

As for adhesion tests, particulate materials were used instead of flat plates (coupons), as model solid materials in this work. Although construction materials used in the food industry are not of a particulate character, the XDLVO model took into account the geometry of the interacting entities. Hence the conclusions made from comparisons of experiments with model predictions (two spheres) are qualitatively valid for any other interaction geometry (plate vs. sphere). The advantage of using model particulate materials with magnetic properties is the ease and reproducible character of quantitative adhesion tests.

In the thermodynamic approach to microbial adhesion, the stability of the surface interaction is expressed as the values of the total free energy of adhesion between cells and solid surfaces in water (ΔG^{TOT}). Adhesion is considered energetically favorable when $\Delta G^{TOT} < 0$, and unfavourable when $\Delta G^{TOT} > 0$. However, the thermodynamic approach does not include the role of long-range electrostatic interactions and therefore it is valid only at close contact (Bos et al. 1999). The free energies of aggregation ($\Delta G^{TOT} > 0$) of the vegetative cells and spores of two *Alicyclobacillus* strains clearly characterize these microorganisms as hydrophilic, while they both show electron donor characteristics ($\gamma^- = 38–81$ mJ m^{-2} vs. $\gamma^+ = 0.2–6.7$ mJ m^{-2} and a predominantly negative ZP (Fig. 1). Another study ranked vegatative cells of six *Alicyclobacillus* strains, by affinity method toward hydrocarbons, in a broad range from very hydrophobic to hydrophilic (do Prado et al. 2018).

The comparison of model predictions with adhesion experiments showed a qualitatively reliable capability of the XDLVO model to predict cell (spore) adhesion to model materials represented by MB. Significant experimental AI was supported by either the absence of an energy barrier or the presence of deep SM in model predictions.

When simulating acidic cleaning (pH 3) or rinsing of solid surfaces with water (pH 7), DEAE-modified surfaces were significantly more prone to interact with cells or spores of the two *Alicyclobacillus* strains. Similar observations were made for anaerobic beer spoiling bacteria (Bittner et al. 2016). The high AI of the *Alicyclobacillus* strains under acidic conditions is particularly disadvantageous, given the facts that the fruit juices have acidic pH and the bacteria are able to survive highly acidic environments (Steyn et al. 2011). In addition, an external pH below 3.6 triggers biofilm formation by *A. acidoterrestris* (Shemesh et al. 2014). There was no significant difference in observed AI between spores and vegetative cells.

Under acidic conditions the main driving force of adhesion was the electrostatic interaction. Neglecting these interactions in a previous study led to ambiguous correlations between hydrophobicity and cell adherence to glass surfaces (Tyfa et al. 2015) and stainless steel (do Prado et al. 2018). At pH 12, both strains showed low ability to interact with all model materials studied, mainly due to the repulsive character of electrostatic interactions. These observations confirmed the XDLVO model, which predicted the crucial importance of EL attractions/repulsions.

After the DEAE surface imitating steel, the second largest AI was predicted and experimentally confirmed to be octyl MB, playing the role of hydrophobic materials. This observation confirmed the results obtained with stainless steel and nylon/polyvinyl chloride (hydrophobic surfaces) as material colonized more extensively (dos Anjos et al. 2013) than glass (hydrophilic surface) (Tyfa et al. 2015). In the case of octyl-modified surfaces (hydrophobic), the main driving forces of adhesion were EL interactions, but at shorter separation distances (< 1 nm), AB interactions prevailed.

Microbial adhesion to solid surfaces and biofilm formation occurs in food processing plants within hours of a cleaning procedure (Storgards et al. 2006). *Alicyclobacillus* was found in fruit processing environments and in water that was used for cleaning and sanitizing purposes (Steyn et al. 2011). A previous study suggested that effective cleaning can be carried out only in a knowledge-based manner taking into consideration the choice of sanitizer (dos Anjos et al. 2013; Bevilacqua et al. 2008). This study defined the appropriate cleaning conditions (pH) and identified the critical materials having greater attractiveness for colonization by *Alicyclobacillus* sp. Since the lowest rate of adhesion between cells/spores of *Alicyclobacillus* sp. and model materials was observed at pH 12, the use of alkaline sanitizers and/or alkaline rinse water can be recommended.

Acknowledgements This research was supported by the Grant Agency of the Czech Republic through project 18-05007S.

References

Abee T, Kovacs AT, Kuipers OP, Veen S (2011) Biofilm formation and dispersal in gram-positive bacteria. Curr Opin Biotech 22:172–179

Azeredo DRP, Alvarenga V, Sant'Ana AS, Sabaa Srur AUO (2016) An overview of microorganisms and factors contributing for the microbial stability of carbonated soft drinks. Food Res Int 82:136–144

Bevilacqua A, Sinigaglia M, Corbo MR (2008) *Alicyclobacillus acidoterrestris*: new methods for inhibiting spore germination. Int J Food Microbiol 125:103–110

Bittner M, de Souza AC, Brozova M, Matoulkova D, Dias DR, Branyik T (2016) Adhesion of anaerobic beer spoilage bacteria *Megasphaera cerevisiae* and *Pectinatus frisingensis* to stainless steel. LWT Food Sci Technol 70:148–154

Bittner M, Strejc J, Matoulkova D, Kolska Z, Pustelnikova T, Branyik T (2017) Adhesion of *Megasphaera cerevisiae* onto solid surfaces mimicking materials used in breweries. J I Brewing 123:204–210

Bos R, van der Mei HC, Busscher HJ (1999) Physico-chemistry of initial microbial adhesive interactions-its mechanisms and methods for study. FEMS Microbiol Rev 23:179–230

Chang SS, Kang DH (2004) *Alicyclobacillus* spp. in the fruit juice industry: history characteristics and current isolation, detection procedures. Crit Rev Microbiol 30:55–74

Chen S, Tang Q, Zhang X, Zhao G, Hu X, Liao X, Chen F, Wu J, Xiang H (2006) Isolation and characterization of thermo-acidophilic endospore-forming bacteria from the concentrated apple juice-processing environment. Food Microbiol 23:439–445

do Prado BD, Fernandes MD, dos Anjos MM, Tognim MCB, Nakamura CV, Machinski M, Mikcha JMG, de Abreu BA (2018) Biofilm-forming ability of *Alicyclobacillus* spp. isolates from orange juice concentrate processing plant. J Food Saf 38:e12466

dos Anjos MM, Ruiz SP, Nakamura CV, de Abreu Filho BA (2013) Resistance of *Alicyclobacillus acidoterrestris* spores and biofilm to industrial sanitizers. J Food Protect 76:1408–1413

Frank JF (2000) Control of biofilms in the food and beverage industry. In: Walker J, Surman S, Jass JH (eds) Industrial biofouling: detection, prevention and control. Wiley, Chichester, pp 205–224

Gispert MP, Serro AP, Colaco R, Saramago B (2008) Bovine serum albumin adsorption onto 316L stainless steel and alumina: a comparative study using depletion, protein radiolabeling, quartz crystal microbalance and atomic force microscopy. Surf Interface Anal 40:1529–1537

Hamouda T, Shih AY, Baker JR Jr (2002) A rapid staining technique for the detection of the initiation of germination of bacterial spores. Lett Appl Microbiol 34:86–90

Huang XC, Yuan YH, Guo CF, Gekas V, Yue TL (2015a) *Alicyclobacillus* in the fruit juice industry: spoilage, detection, and prevention/control. Food Rev Int 31:91–124

Huang Q, Yang Y, Hu R, Lin C, Sun L, Vogler EA (2015b) Reduced platelet adhesion and improved corrosion resistance of superhydrophobic TiO_2-nanotube-coated 316L stainless steel. Colloid Surf B 125:134–141

Israelachvili JN (2011) Intermolecular and surface forces. Academic Press, London

McKnight IC, Eiroa MNU, Sant'Ana AS, Massaguer PR (2010) *Alicyclobacillus acidoterrestris* in pasteurized exotic Brazilian fruit juices: isolation, genotypic characterization and heat resistance. Food Microbiol 27:1016–1022

Olszewska MA (2013) Microscopic findings for the study of biofilms in food environments. Acta Biochim Pol 60:531–537

Peng JS, Tsai WC, Chou CC (2002) Inactivation and removal of *Bacillus cereus* by sanitizer and detergent. Int J Food Microbiol 77:11–18

Pettipher GL, Osmundson M, Murphy J (1997) Methods for the detection and enumeration of *Alicyclobacillus acidoterrestris* and investigation of growth and production of taint in fruit juice and fruit juice-containing drinks. Lett Appl Microbiol 24:185–189

Prochazkova G, Podolova N, Safarik I, Zachleder V, Branyik T (2013) Physicochemical approach to freshwater microalgae harvesting with magnetic particles. Colloid Surf B 112:213–218

Redman JA, Walker SL, Elimelech M (2004) Bacterial adhesion and transport in porous media: role of the secondary energy minimum. Environ Sci Technol 38:1777–1785

Sauer K (2003) The genomics and proteomics of biofilm formation. Genome Biol 4:219

Sharma PK, Hanumantha Rao K (2002) Analysis of different approaches for evaluation of surface energy of microbial cells by contact angle goniometry. Adv Colloid Interfac 98:341–463

Shemesh M, Pasvolsky R, Zakin V (2014) External pH is a cue for the behavioral switch that determines surface motility and biofilm formation of *Alicyclobacillus acidoterrestris*. J Food Prot 77:1418–1423

Smit Y, Cameron M, Venter P, Witthuhn RC (2011) *Alicyclobacillus* spoilage and isolation—a review. Food Microbiol 28:331–349

Spinelli ACNF, Sant'Ana AS, Pacheco-Sanchez CP, Massaguer PR (2010) Influence of the hot-fill water-spray-cooling process after continuous pasteurization on the number of decimal reductions and on *Alicyclobacillus acidoterrestris* CRA 7152 growth in orange juice stored at 35 °C. Int J Food Microbiol 137:295–298

Srey S, Jahid IK, Ha SD (2013) Biofilm formation in food industries: a food safety concern. Food Control 31:572–585

Steyn CE, Cameron M, Witthuhn RC (2011) Occurrence of *Alicyclobacillus* in the fruit processing environment—a review. Int J Food Microbiol 147:1–11

Storgards E, Tapani K, Hartwall P, Saleva R, Suihko ML (2006) Microbial attachment and biofilm formation in brewery bottling plants. J Am Soc Brew Chem 64:8–15

Tianli Y, Jiangbo Z, Yahong Y (2014) Spoilage by *Alicyclobacillus bacteria* in juice and beverage products: chemical, physical, and combined control methods. Compr Rev Food Sci F 13:771–797

Tyfa A, Kunicka-Styczynska A, Zabielska J (2015) Evaluation of hydrophobicity and quantitative analysis of biofilm formation by *Alicyclobacillus* sp. Acta Biochim Pol 62:785–790

van Oss CJ (1995) Hydrophobicity of biosurfaces–origin, quantitative determination and interaction energies. Colloid Surf B 5:91–110

van Oss CJ (2003) Long-range and short-range mechanisms of hydrophobic attraction and hydrophilic repulsion in specific and aspecific interactions. J Mol Recognit 16:177–190

van Oss CJ (2006) Interfacial forces in aqueous media. CRC Press, Boca Raton